

STARCH/POLY (BUTYLENE ADIPATE–CO-TEREPHTHALATE)/MONTMORILLONITE FILMS PRODUCED BY BLOW EXTRUSION**Rodrigo A. L. Santos^a, Carmen M. O. Muller^a, Maria V. E. Grossmann^a, Suzana Mali^{b,*} and Fabio Yamashita^a**^aDepartamento de Ciência e Tecnologia de Alimentos, Centro de Ciências Agrárias, Universidade Estadual de Londrina, 86057-970 Londrina – PR, Brasil^bDepartamento de Bioquímica e Biotecnologia, Centro de Ciências Exatas, Universidade Estadual de Londrina, 86051-990 Londrina – PR, Brasil

Recebido em 03/07/2013; aceito em 24/03/2014; publicado na web em 17/06/2014

This study aims to prepare biodegradable films from cassava starch, poly (butylene adipate–co-terephthalate) (PBAT), and montmorillonite (MMT) using blow-extrusion process and analyze the effects of different types and concentrations of MMT on the microstructure, physicochemical, and mechanical properties of the resulting films. The films were produced by blending 30% of PBAT with glycerol (17.5%), starch (49.0–52.5%), and four different types of montmorillonite (Cloisite® Na⁺, 10A, 15A, and 30B) at two different concentrations (1.75% and 3.5%). All the films prepared in this study showed an increase in the basal spacing of MMT layers. In particular, the films with 10A and 30B showed the highest increase in intercalation basal spacing, suggesting the formation of intercalated composites. The addition of nanoclays decreased the elongation of films. The addition of Cloisite® 10A resulted in films with the lowest WVP values and the highest stability to water adsorption under different RH conditions.

Keywords: biodegradable films; nanoclays; intercalated nanocomposites.

INTRODUCTION

Plastic resins are widely used in packaging materials as potential alternatives to glass- and metal-based materials, owing to their low weight and manufacturing versatility. However, the increased use of plastic-based packaging materials has brought about environmental concerns associated with the non-degradability of plastic wastes. To overcome these problems, several studies have focused on the development of biodegradable plastic, aiming at research and development of sustainable packaging materials, particularly in the form of starches, agro-resources, and co-polyesters.^{1,2}

Among these biodegradable materials, thermoplastic starch has attracted considerable attention. Although it has some drawbacks, such as poor water resistance and comparatively poor mechanical properties, these shortcomings could be circumvented by blending these materials with synthetic co-polyester biodegradable polymers. Blending starch with other biodegradable polymers, such as polyhydroxybutyrate (PHB), poly (lactic acid) (PLA), poly (ε-caprolactone) (PCL), poly (butylene succinate–co-adipate) (PBSA), polyvinyl alcohol (PVOH), and poly (butylene adipate–co-terephthalate) (PBAT) may reduce the production costs, making them more competitive when compared to conventional packaging materials.³

Yet another viable approach to improve the mechanical and permeation properties of starch materials is the use of nanometer-scale additives. Although several nanoparticles have been recognized as additives with the potential to enhance the polymer performance, most intensive studies are currently focused on layered silicate minerals, such as montmorillonite (MMT). This class of minerals has high availability, high versatility, and low cost, besides being benign in terms of environment and human health.⁴ The MMT crystal lattice consists of ultrathin (1 nm) layers of octahedral alumina sheets sandwiched between sheets of tetrahedral silica. Each of these layers is negatively charged, and the excess charge is balanced by alkali cations, such as Na⁺, Li⁺ or Ca²⁺, that reside in the gallery space between

the aluminosilicate layers.^{5,6} To improve their dispersibility, clays are often modified with organic surfactants, which are typically the quaternary ammonium salts of long fatty acid chains. These surfactants decrease the surface tension of the aluminosilicate particulates, which in turn reduces the endothermic enthalpy of mixing. To this end, several organophilic nanoclays are being studied, and some of their products are already being marketed on an industrial scale.^{7,8}

The objectives of the present study are to develop biodegradable films from cassava starch, PBAT, and four different types of montmorillonite by using the blow-extrusion process, and to study the effects of the different types and concentrations of MMT on the microstructure, physicochemical, and mechanical properties of the resulting films.

EXPERIMENTAL**Materials**

Biodegradable films were manufactured using cassava starch (Indemil - Paranavaí - Brazil) and glycerol (Synth - Brazil). The biodegradable polyester used in this study was poly (butylene adipate–co-terephthalate), which is produced by BASF under the trade name Ecoflex® S BX 7025. The nanoclays were obtained from Southern Clay Products, Inc. (USA). The four different types of MMT used in this study are: unmodified montmorillonite (Cloisite® Na⁺) and three types of organically modified montmorillonite, namely, Cloisite® 10A, 15A, and 30B, with cation exchange capacities of 125, 125 and 90 meq/100 g, respectively.

Methods*Film production*

In the typical process adopted for the synthesis of biodegradable film, each type of MMT was mixed with glycerol under vigorous stirring for 10 min, followed by the addition of PBAT and starch using a mechanic stirrer at 18,000 rpm (Vithory-Brazil). These blended

*e-mail: smali@uel.br

materials were pelletized in a single-screw pilot extruder (BGM model EL-25, Brazil) at 45 rpm at the temperatures of 120, 130, 125, and 115 °C along the four barrel zones of the extruder. These pellets were extruded again for film production by blowing (100-mm circular blowing matrix diameter) at 45 rpm at the temperatures of 120, 120, 115, and 120 °C along the four barrel zones, and at the temperature of 130 °C in the annular matrix of the extruder. The films were manufactured using different formulations that are optimized on the basis of our previous study (results not been published). The formulations adopted for the manufacturing of the films are summarized in Table 1. The starch content ranged from 49.0 to 52.5%, the MMT content ranged from 0 to 3.50%, and the glycerol and PBAT contents were fixed at 17.5 and 30.0%, respectively. The film specimens were denominated as follows: nanoclay name + nanoclay concentration.

Table 1. Formulations adopted for the preparation of biodegradable films

Film specimens ^a	Nanoclay (%)	Starch + Glycerol (%)	PBAT (%)	TOTAL (%)
Control	0	52.50 + 17.5	30	100
Na1.75%	1.75	50.75 + 17.5	30	100
10A1.75%	1.75	50.75 + 17.5	30	100
15A1.75%	1.75	50.75 + 17.5	30	100
30B1.75%	1.75	50.75 + 17.5	30	100
Na3.5%	3.50	49.00 + 17.5	30	100
10A3.5%	3.50	49.00 + 17.5	30	100
15A3.5%	3.50	49.00 + 17.5	30	100
30B3.5%	3.50	49.00 + 17.5	30	100

^aNa1.75% and Na3.5% (formulated with Cloisite® Na⁺), 10A1.75% and 10A3.5% (formulated with Cloisite® 10A), 15A1.75% and 15A3.5% (formulated with Cloisite® 15A), 30B1.75% and 30B3.5% (formulated with Cloisite® 30B).

Films characterization

Thickness, density, and opacity

The thickness of the resulting films was measured using a manual micrometer (Mitutoyo, Japan). For each formulation, the reported value of thickness is the average of 3 measurements obtained from 5 test samples. Furthermore, the density was calculated as the quotient of the weight divided by the volume of the dried samples. The reported density values are the average of 7 measurements for each formulation. The opacity of the resulting films was determined using a BYK Gardner colorimeter, according to the method reported by Sobral.⁹ The opacity of the sample was compared to a white (Y_w) and a black (Y_b) standard, according to the equation: $Y = (Y_b/Y_w) * 100$. The results were given as the percentage of opacity. All the opacity tests were conducted in triplicate.

X-ray diffraction analysis (XRD)

The diffraction patterns of the films were recorded on a PANalytical X'Pert PRO multi-purpose diffractometer (Netherlands) using copper K α radiation ($\lambda = 1.5418 \text{ \AA}$) under operational conditions of 40 kV and 30 mA. Prior to analysis, the samples were previously conditioned at 25 °C for 72 h under the RH value of 64%. The d_{001} spacing was calculated by first determining the 2θ value for the scattering peak, followed by the substitution of the 2θ value in the Bragg's equation.¹⁰ The relative intercalation (RI) of the nanoclays in the films was quantified as $RI = ((d - d_0)/(d_0)) * 100$, where d is the interlayer or d -spacing of the nanoclay in the films and d_0 is the d -spacing of the pure nanoclay.¹⁰ The crystallinity index (CI) of the

samples was calculated as the ratio between the crystalline area and the total area of the XRD pattern, according to the method reported by Rulland.¹¹ The Origin 8.0 software package (Origin Lab Corporation, MA, USA) was used to calculate the areas.

Fourier Transform-Infrared Spectroscopy (FT-IR)

The FT-IR spectra of the nanocomposite films were recorded on a Bomem FT-100 Fourier-transform infrared spectrometer (Switzerland) equipped with an attenuated total reflectance Pike Miracle™ HATR in the wavelength range of 400–4000 cm^{-1} , at the spectral resolution of 4 cm^{-1} at the rate of 16 scans per sample. Prior to analysis, the samples were dehydrated in desiccators containing calcium chloride (CaCl₂) for 15 d at 25 °C.

Mechanical properties

The mechanical properties of the films were determined from tension tests using the TA-XT2i texture analyzer (England), in accordance with the ASTM 882-02 standards.¹² Samples were clamped between grips, and the force and deformation were recorded during extension at 50 mm/min, with an initial distance of 50 mm between the grips. Thus, the tensile strength (MPa) and elongation (%) were determined from ten replicates for each film formulation. Prior to analysis, the samples were pre-conditioned at 25 °C for 72 h at the RH value of 64%.

Water vapor permeability (WVP)

The WVP of the films was determined in appropriate diffusion cells (ASTM E96-00)¹³ using three different relative humidity (RH) gradients (0–33%, 33–64%, 64–90%). The salt solutions (33% - magnesium chloride, 64% - sodium nitrate and 90% - barium chloride) and held at 25 °C (Rockland, 1960) were prepared according to procedure reported by Rockland.¹⁴ In the typical process, the films were fixed into the openings of the cells containing the salt solution, which provided a lower relative humidity (0%, 33% or 64%, depending on the case). Subsequently, they were placed in a hermetic chamber containing the salt solution, which provided a higher relative humidity (33, 64 or 90%, depending on the case). The chamber with the diffusion cells was kept at 25 °C, and the corresponding weight gain was recorded and plotted as a function of time. The slope of each line was calculated by linear regression ($r^2 > 0.99$), and the water vapor transmission rate (WVTR) was calculated from the slope of the straight line (g/s) divided by the transport area (m^2). The WVP ($\text{g Pa}^{-1} \text{ s}^{-1} \text{ m}^{-1}$) was calculated using the expression $WVP = [WVTR/S (R_1 - R_2) * D]$, where S is the saturation vapor pressure of water (Pa) at the given temperature (25 °C), R_1 is the RH inside the desiccator, R_2 is the RH inside the permeation cell, and D is the thickness of the film (m). All the tests were conducted in triplicate.

Water sorption isotherms

The moisture sorption isotherms of the films were determined by the static method using saturated saline solutions (11% - lithium chloride, 32% - magnesium chloride, 43% - potassium carbonate, 58% - sodium bromide, 64% - sodium nitrate, 75% - sodium chloride, and 90% - barium chloride) held at 25 °C to obtain different relative humidities.¹⁵ The starch films specimens (2.0 x 2.0 cm) were pre-dried for 14 days over anhydrous calcium chloride, and were then placed at 25 °C over saturated salt solutions in separate desiccators with the desired levels of relative humidity (11, 32, 43, 53, 64, 75, and 90%).¹⁴ Each film specimen was weighed at regular intervals (a minimum of 6 h and a maximum of 12 h), and equilibrium was assumed to be reached when two consecutive measurements were equal. Under the abovementioned conditions, an equilibrium period of 14 d was sufficient to establish equilibrium in all samples. The

equilibrium moisture content was calculated from the increase in the mass of the dried sample upon achieving equilibrium at a given RH. All the tests were conducted in triplicate.

Statistical analysis

Analyses of variance (ANOVA) and Tukey tests ($p \leq 0.05$) were performed using Statistica 6.0 software (STATSOFT, 2001).

RESULTS AND DISCUSSION

Thickness, density, and opacity

The formulations were blown into films without any difficulties, and none of the films presented a sticky surface during or immediately after the extrusion process (Figure 1S - Supplementary Material). All the formulations adopted for manufacturing the films resulted in films with good resistance for handling, folding and crushing. None of the samples showed resistance to shredding. The addition of nanoclay did not affect the thickness, density, or opacity of the films (Table 2). A high concentration of nanoclay resulted in a slight increase in the density and opacity, although not significant. According to Chen *et al.*,¹⁶ the transparency of the film provides information about the compatibility of the film components. Accordingly, the nanometer-sized particles could potentially interact and improve the transparency of the starch films.

Table 2. Thickness, density, and opacity of the extruded films

Film specimens	Thickness (μm)	Density (g/cm^3)	Opacity (%)
Control	124 \pm 23 a	1.14 \pm 0.02 a	56.2 \pm 3.3 a
Na 1.75%	125 \pm 25 a	1.16 \pm 0.06 a	53.9 \pm 2.7 a
10A 1.75%	125 \pm 25 a	1.20 \pm 0.05 a	56.8 \pm 2.9 a
15A 1.75%	131 \pm 25 a	1.18 \pm 0.06 a	57.0 \pm 2.3 a
30B 1.75%	125 \pm 21 a	1.17 \pm 0.05 a	57.3 \pm 2.3 a
Na 3.5%	140 \pm 29 a	1.22 \pm 0.07 a	58.7 \pm 3.4 a
10A 3.5%	127 \pm 37 a	1.22 \pm 0.02 a	59.2 \pm 3.9 a
15A 3.5%	141 \pm 41a	1.23 \pm 0.05 a	58.2 \pm 4.0 a
30B 3.5%	127 \pm 39 a	1.23 \pm 0.04 a	60.1 \pm 3.9 a

Different letters in the same column indicate significant differences ($p \leq 0.05$) between means (Tukey test).

XRD analysis

According to previous studies,^{17,18} cassava starch has a C-type crystalline structure with peaks at 2θ corresponding to 15.3° , 17.3° , 18.3° , 22° , and 23.5° , as seen in the diffraction pattern of the control film shown in Figure 1. Although some of the diffraction peaks disappeared as a consequence of starch gelatinization during the extrusion process, other peaks still appeared in the diffraction pattern.

The peaks at 17.43° and 22.8° seen in the diffraction pattern of the control film are the characteristic peaks of PBAT.¹⁹ The peak at $2\theta = 19^\circ$ could possibly correspond to the process-induced crystallinity. According to Van Soest and Vliegthart,²⁰ this peak corresponds to the V_A -type crystallinity of thermoplastic starch. This type of crystallinity is also associated with the amylose recrystallization induced during the extrusion process. Few other studies have reported this type of crystallinity in extruded starch materials with low moisture content.^{21,22}

Figure 2 shows the X-ray diffraction patterns of the composite films, and Table 3 shows the interlayer spacing corresponding to the major peaks of the composite films and pure nanoclays. As is seen,

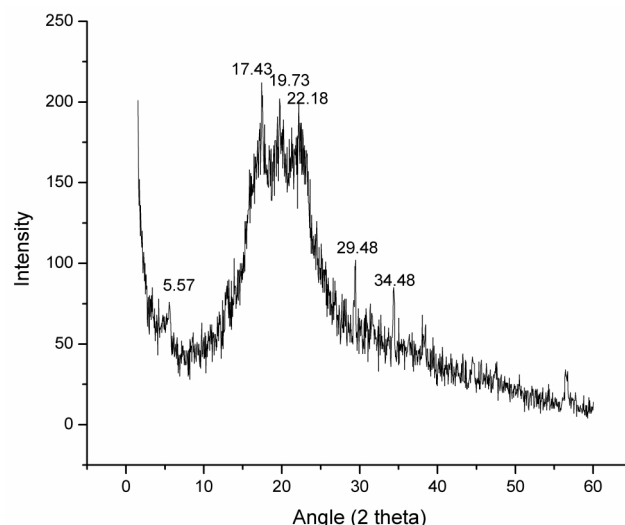


Figure 1. X-ray diffraction pattern of the control film

all the composite films showed an increase in the basal spacing of MMT layers, with the films containing the 30B nanoclays showing the highest basal spacing of MMT layers and highest relative intercalation (Table 3; Figure 2). Besides, the 10A and Na films also showed high relative intercalation values of 59.64 and 48.80%, respectively. These results suggest the possible intercalation of the starch or PBAT polymer chains into the silicate layers, forming intercalated composites without complete exfoliation. Several studies have associated the increase of interlayer distance to the formation of intercalated structure in polymers and nanoclay composites.^{7,23,24} During melt intercalation, the insertion of the polymer into the organoclay galleries forces the platelets apart and increases the d-spacing, resulting in a shift of the diffraction peak to lower angles.²⁵

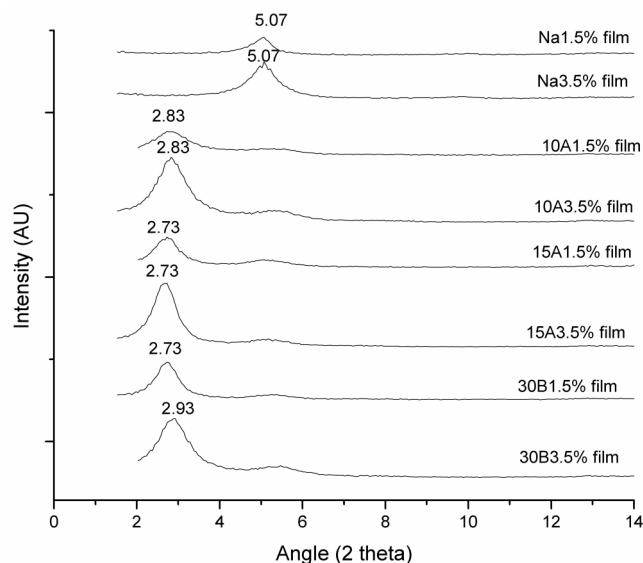


Figure 2. X-ray diffraction patterns of starch-PBAT-nanoclay films

Among all the clays produced by Southern Clay Products (Cloisite[®] Na⁺, 10A, 15A, and 30B), Cloisite Na⁺ is the most hydrophilic and 15A is the most hydrophobic clay. Cloisite 30B and 10A have intermediate hydrophobicity, with 10A being more hydrophobic than 30B.²⁶ Therefore, it is likely that the higher hydrophobicity of the 15A clay did not favor the chemical interaction with the hydrophilic polymeric chain of starch.

Table 3. Major peaks angles, d-spacings, relative intercalation (RI), and crystallinity index (CI) of pure nanoclays and extruded films

Films specimens	Films ^a		Pure Nanoclay ^a		Difference (d - d ₀) Film-MMT (Å)	RI (%)	CI (%)
	Peak (2θ)	d-spacing (Å)	Peak (2θ)	d ₀ -spacing (Å)			
Control	-	-	-	-	-	-	20.15
Na 1.75%	5.07	17.41	7.85	11.7	5.71	48.80	21.38
10A 1.75%	2.83	30.65	4.52	19.2	11.45	59.64	25.40
15A 1.75%	2.73	32.33	2.80	31.5	0.83	2.63	25.14
30B 1.75%	2.73	32.33	4.73	18.5	13.83	74.76	31.10
Na 3.5%	5.07	17.41	7.85	11.7	5.71	48.80	26.33
10A 3.5%	2.83	30.65	4.52	19.2	11.45	59.64	29.40
15A 3.5%	2.73	32.33	2.80	31.5	0.83	2.63	39.09
30B 3.5%	2.93	30.12	4.73	18.5	11.62	62.81	29.53

^aValues obtained from experimental XRD patterns.

The crystallinity index (CI) of the films ranged from 20.15 to 39.09% (Table 3). The addition of nanoclay to the starch matrix increased the crystallinity of the material when compared to the control sample. This behavior has also been reported in hybrid starch and nanoclay composites.^{2,27,28} An increase in the concentration of nanoclay from 1.75 to 3.50% resulted in higher CI values for all the clays except 30B (Table 3).

Fourier Transform-Infrared Spectroscopy (FT-IR)

The FT-IR spectra of all the film specimens (Figure 3) showed an absorption band in the wavelength range of 3200–3500 cm⁻¹, corresponding to O–H bond stretching. The presence of this band could possibly be attributed to the existence of H-bonding interactions between the film components during the manufacturing process.

In general, free O–H band of the pure nanoclay surface²⁹ shows an absorption band at around 3627 cm⁻¹. However, all the film samples prepared in the present study showed a shift of this band (Figure 3) to a lower frequency of around 3400 cm⁻¹, characteristic of the hydroxyl groups that participate in the formation of hydrogen bonds. This is indicative of the possible interaction between starch, PBAT, and MMT. Similar observations have been previously reported by other authors.^{30,31}

The FT-IR spectra of pure nanoclays show a strong absorption band at around 1030 cm⁻¹, corresponding to the Si–O stretching vibrational modes.³² However, this band could not be observed (Figure 3) in any of the films prepared with the addition of nanoclay, except for the 30B3.5% film, in which the relative intensity of this band was lower when compared to the untreated film. These results indicate the intercalation of the clays with the polymeric matrix, as discussed earlier in the XRD analysis.

The FT-IR peak at around 1720 cm⁻¹ could be ascribed to carbonyl stretching, while the band at 2940 cm⁻¹ corresponds to the carboxyl OH stretching. These results confirm the formation of carboxylic acid groups as a result of the chemical reaction between PBAT, TPS, and nanoclays. Mohanty and Nayak³³ have reported similar results in starch-based biodegradable nanocomposites of PBAT and organically modified nanoclays.

Mechanical properties

As can be seen from the results summarized in Table 4, the addition of nanoclay does not affect the tensile strength of the resulting films. Rather, only the films produced with the low CloisiteNa⁺ concentration (Na1.75% sample) show a significant increase in tensile

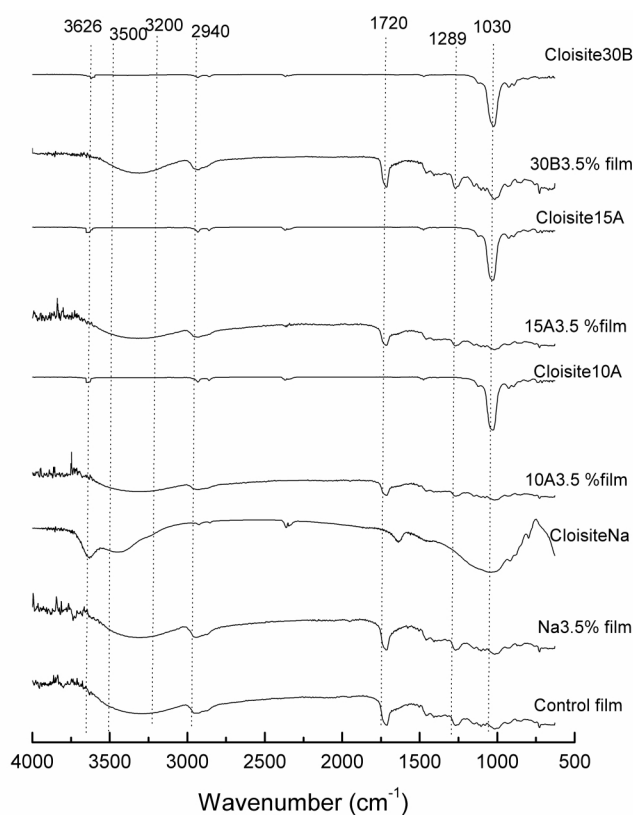


Figure 3. FT-IR spectra of pure nanoclays and starch-PBAT-nanoclay films

strength when compared to the control films. It could possibly be attributed to the concentration of nanoclays used in this study that is not sufficient enough to increase the tensile strength of our samples. According to the study reported by Faruk and Matuana,¹⁰ the clay concentration of less than 10 wt.% is effective in improving the mechanical and barrier properties of the plastics. Therefore, it is possible that the use of nanoclay in the concentration range of 3.5–10 wt.% could have resulted in better results.

As observed in Table 3, the elongation of the films decreased with the addition of nanoclays (Table 4). All the films prepared in this study showed an intercalated structure, which could have resulted in more rigid polymeric matrices with lower elongation values. These results are in good agreement with those reported in previous studies.^{2,5} According to Ardakani *et al.*,⁵ the existence of greater gallery spacing is indicative of the diffusion of more starch or PBAT molecules

Table 4. Mechanical properties and water vapor permeability of the extruded films

Film sample	Mechanical Properties		WVP (g/m day Pa) × 10 ⁶		
	Tensile strength (MPa)	Elongation (%)	ΔRH (2 - 33%)	ΔRH (33 - 64%)	ΔRH (64 - 90%)
Control	5.58 ± 1.00 a,b	325 ± 80 a	3.13 ± 0.17 b	7.48 ± 0.50 b	15.05 ± 1.23 a
Na1.75%	6.20 ± 0.90 a	250 ± 72 b	2.38 ± 0.15 c	10.43 ± 1.09 a	14.71 ± 2.46 a
10A1.75%	5.58 ± 1.02 a,b	220 ± 75 b	2.18 ± 0.13 c	6.82 ± 0.12 b,c	13.49 ± 1.53 a
15A1.75%	5.60 ± 0.98 a,b	215 ± 68 b	2.20 ± 0.08 c	7.60 ± 0.56 b	15.74 ± 1.29 a
30B1.75%	4.90 ± 0.70 b	250 ± 70 b	2.54 ± 0.04 c	6.99 ± 0.52 b	14.28 ± 1.95 a
Na3.5%	5.75 ± 0.82 a,b	175 ± 35 c	2.29 ± 0.36 c	9.32 ± 0.23 a	16.02 ± 3.55 a
10A3.5%	5.50 ± 0.75 a,b	225 ± 65 b	1.28 ± 0.12 d	6.48 ± 0.59 c	14.50 ± 2.13 a
15A3.5%	5.75 ± 0.72 a,b	200 ± 55 b,c	2.67 ± 0.11 c	9.50 ± 0.35 a	17.04 ± 3.95 a
30B3.5%	5.48 ± 0.69 a,b	250 ± 89 a,b	3.91 ± 0.11 a	7.85 ± 0.97 b	16.69 ± 4.21 a

Different letters in the same column indicate significant differences ($p \leq 0.05$) between means (Tukey test).

into the space between the silicate layers. This, in turn, increases the interfacial interactions, leading to more intensive reinforcing effects.

Notably, the tensile strength of the films prepared in this study ranged from 4.90–6.20 MPa (Table 4). Although it is considered lower, it is still comparable to the tensile strength values reported for low density polyethylene (LDPE) films (8.34 MPa).³⁴ The elongation values of the films prepared in this study (Table 4) were approximately half of those of the LDPE films, which have an elongation of approximately 600%.³⁴

Water vapor permeability

The water vapor permeability of the films was determined at three gradients of relative humidity (ΔRH), namely 0–33%, 33–64%, 64–90%, with different absolute values of RH, to understand the hygroscopic behavior of the films. As can be seen from the results summarized in Table 4, the WVP of the films increase with the absolute values of RH. These results are in good agreement with the previous study³⁵ on the WVP of cassava starch films determined under the same RH gradients used in the present work. According to the previous study, WVP is controlled by the solubility coefficient of water in the films. Under higher absolute values of RH, this coefficient increases and results in higher water permeation through the films.

The addition of nanoclays decreased the WVP of all the films under the RH gradients of 0–33% and 33–64%, except for the specimen 30B3.5% (Table 4). Under the RH gradient of 64–90%, the addition of nanoclays did not affect the WVP of the films.

In principle, the nanoclay lamellae are distributed in the polymer matrix, forcing the vapor to flow through a tortuous path, thereby forming a complex barrier system. The higher the tortuosity of the system, the better the barrier properties.²⁶

In the present study, the film with the lowest WVP was the 10A3.5% at ΔRH (0–33%) and at ΔRH (33–64%). It is clear that the intercalation effect increases the tortuosity of the path of the water molecule and decreases the permeability of these films.²⁶

Moisture sorption isotherms

Figure 4 shows the moisture sorption isotherms of the films prepared in this study. As is seen, all the films present similar sigmoidal isotherm patterns. The equilibrium moisture content of the samples increases with increase in relative humidity. In particular the increase in equilibrium moisture was more pronounced when the samples were stored at an RH above 75%. This behavior is interesting because the main problem with these materials is their sensitivity to moisture.^{31,36}

When the films were stored in RH between 11 and 75%, the equilibrium moisture content was not affected by the film formulation (Figure 4). However, the specimen 10A3.5% presented the lowest water uptake at RH of 43, 53, 75, 85, and 90%, when compared with other films. This is indicative of the existence of a more stable polymeric matrix. Besides, this film formulation also showed the lowest WVP values at two different RH gradients (ΔRH (0–33%) and ΔRH (33–64%).

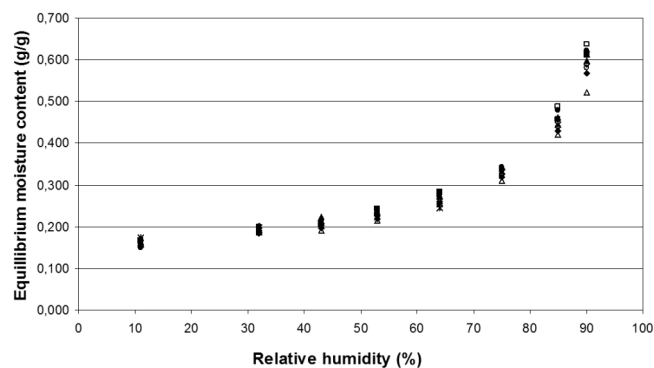


Figure 4. Water sorption isotherms of the films: control (*), Na.175% (■), Na3.5% (□), 10A1.75% (▲), 10A3.5% (△), 15A 1.75% (●), 15A3.5% (○), 30B1.75% (◆), 30B3.5% (◇)

CONCLUSIONS

In summary, all the films prepared in this study were continuous (rupture-free), homogeneous (free of insoluble particles and bubbles), easy to handle, and showed ease of processability during the blow extrusion process. The nanoclays with intermediate hydrophobicity (Cloisite® 10A and 30 B) favored the formation of films with higher basal spacing of the layered silicates and higher relative intercalation rates. This is indicative of the strong interaction between the polymeric matrix and the nanoclay, suggesting that the starch polymer chains enter into the silicate layers forming intercalated composites without complete exfoliation. The addition of nanoclay did not affect the tensile strength of the resulting films, although it decreased the elongation of the films. The addition of Cloisite® 10A resulted in films with the lowest WVP values under the RH gradients of 0–33% and 33–64%. Besides, the 10A films were more stable to water adsorption under a range of RH conditions. Further developments are needed to improve the interaction between the polymeric matrix and the nanoclay to form an exfoliated structure. However, the preliminary

results presented in this study substantiate that fact that the addition of nanoclay is a promising approach for industrial-scale manufacturing of starch-based films.

SUPPLEMENTARY MATERIAL

Figure 1S shows the representative image of the film (Na1.75% film) formed by blown extrusion. The other films were also similar.

ACKNOWLEDGMENTS

The authors acknowledge the final support provided by the Conselho Nacional de Desenvolvimento Científico e Tecnológico (CNPq No. 479768-2012-9), Brazil.

REFERENCES

1. Averous L.; Boquillon, N.; *Carbohydr. Polym.* **2004**, *56*, 111.
2. Müller, C. M. O.; Yamashita, F.; Laurindo, J. B.; *Carbohydr. Polym.* **2012**, *89*, 504.
3. Brandelero, R. P. H.; Grossmann, M. V. E.; Yamashita, F.; *Carbohydr. Polym.* **2011**, *86*, 1344.
4. Azeredo, H. M. D.; *Food Res. Int.* **2009**, *42*, 1240.
5. Ardakani, M. M.; Mohseni, M. A.; Beitollahi, H.; Benvidi, A.; Naeimi, H.; *Chinese Chem. Lett.* **2010**, *21*, 1471.
6. Ray, S. S.; Okamoto, M.; *Prog. Polym. Sci.* **2003**, *28*, 1539.
7. Park, H. W.; Jim, C. Z.; Park, C. Y.; Cho, W. J.; Ha, C. S.; *Macromol. Mater. Eng.* **2002**, *287*, 553.
8. Turri, S.; Alborghetti, L.; Levi, M.; *J. Polym. Res.* **2008**, *15*, 365.
9. Sobral, P. J. A.; *Pesq. Agropec. Bras.* **2000**, *35*, 1.
10. Faruk, O.; Matuana, L. M.; *Compos. Sci. Technol.* **2008**, *68*, 2073.
11. Ruland, W.; *Acta Crystallogr.* **1961**, *14*, 1180.
12. ASTM 882-02. **2002**. Standard test methods for tensile properties of thin plastic sheeting.
13. ASTM E 96-00. **2002**. Standard test methods for water vapor transmission of materials.
14. Rockland, L. B.; *Anal. Chem.* **1960**, *32*, 1375.
15. Bell, L. N.; Labuza, T. P.; *Moisture sorption: Practical aspects of isotherm measurement and use*, AACC Egan Press: Egan, 2000.
16. Chen, Y.; Cao, X.; Chang, P. R.; Huneault, M. A.; *Carbohydr. Polym.* **2008**, *73*, 8.
17. Camargo, C.; Colonna, P.; Buléon, A.; Molar, R. D.; *J. Food Agric.* **1998**, *45*, 273.
18. Zobel, H. F.; *Starch/Staerke* **1998**, *40*, 44.
19. Chivrac, F.; Kadlecova, Z.; Pollet, E.; Averous, L.; *J. Polym. Environ.* **2006**, *14*, 393.
20. Van Soest, J. J. G.; Vliegthart, J. F. G.; *Trends Biotechnol.* **1997**, *15*, 208.
21. Hulleman, S. H. D.; Kalisvaart, M. G.; Janssen, F. H. P.; Feil, H.; Vliegthart, J. F. G.; *Carbohydr. Polym.* **1999**, *39*, 351.
22. Rindlav, A., Hulleman, S. H. D., Gatenholm, P.; *Carbohydr. Polym.* **1997**, *34*, 25.
23. Ma, X.; Yu, J.; Kennedy, J. F.; *Carbohydr. Polym.* **2005**, *62*, 19.
24. Chivrac, F.; Angellier-Coussy, H.; Guillard, V.; Pollet, E.; Averous, L.; *Carbohydr. Polym.* **2010**, *82*, 128.
25. Lee, S. Y.; Chen, H.; Hanna, M. A.; *Ind. Crop. Prod.* **2008**, *28*, 95.
26. Chiou, B. S.; Yee, E.; Glenn, G. M.; Orts, W. J.; *Carbohydr. Polym.* **2005**, *59*, 467.
27. Huang, J.; Schols, H. A.; Van Soest, J. J. G.; Jin, Z.; Sulmann, E.; Vora-gen, A.G.; *J. Food Chem.* **2007**, *101*, 1338.
28. Magalhães, N. F.; Andrade, C. T.; *Carbohydr. Polym.* **2009**, *75*, 712.
29. Field, L. D.; Sternhell, S.; Kalman, J. R.; *J. Chem. Educ.* **2002**, *79*, 11.
30. Liu, H.; Chaudhary, D.; Yusa, S.; Tadé, M. O.; *Carbohydr. Polym.* **2011**, *83*, 1591.
31. Vercelheze, A. E. S.; Fakhouri, F. M.; Dall'Antônia, L. H.; Urbano, A.; Youssef, A. E.; Yamashita, F.; Mali, S.; *Carbohydr. Polym.* **2012**, *87*, 1302.
32. Leite, I. F.; Raposo, C.M.O.; Silva, S. M. L.; *Cerâmica* **2008**, *54*, 303.
33. Mohanty, S.; Nayak, S. K.; *Int. J. Plast. Technol.* **2010**, *13*, 163.
34. Arvanitoyannis, I.; Biliaderis, C. G.; Ogawa, H.; Kawasaki, N.; *Carbohydr. Polym.* **1998**, *36*, 89.
35. Müller, C. M. O.; Yamashita, F.; Laurindo, J. B.; *Carbohydr. Polym.* **2008**, *72*, 82.
36. Mali, S.; Grossmann, M. V. E.; García, M. A.; Martino, M. M.; Zaritzky, N. E.; *J. Food Eng.* **2006**, *55*, 453.

STARCH/POLY (BUTYLENE ADIPATE-CO-TEREPHTHALATE)/MONTMORILLONITE FILMS PRODUCED BY BLOW EXTRUSION

Rodrigo A. L. Santos^a, Carmen M. O. Muller^a, Maria V. E. Grossmann^a, Suzana Mali^{b,*} and Fabio Yamashita^a

^aDepartamento de Ciência e Tecnologia de Alimentos, Centro de Ciências Agrárias, Universidade Estadual de Londrina, 86057-970 Londrina – PR, Brasil

^bDepartamento de Bioquímica e Biotecnologia, Centro de Ciências Exatas, Universidade Estadual de Londrina, 86051-990 Londrina – PR, Brasil

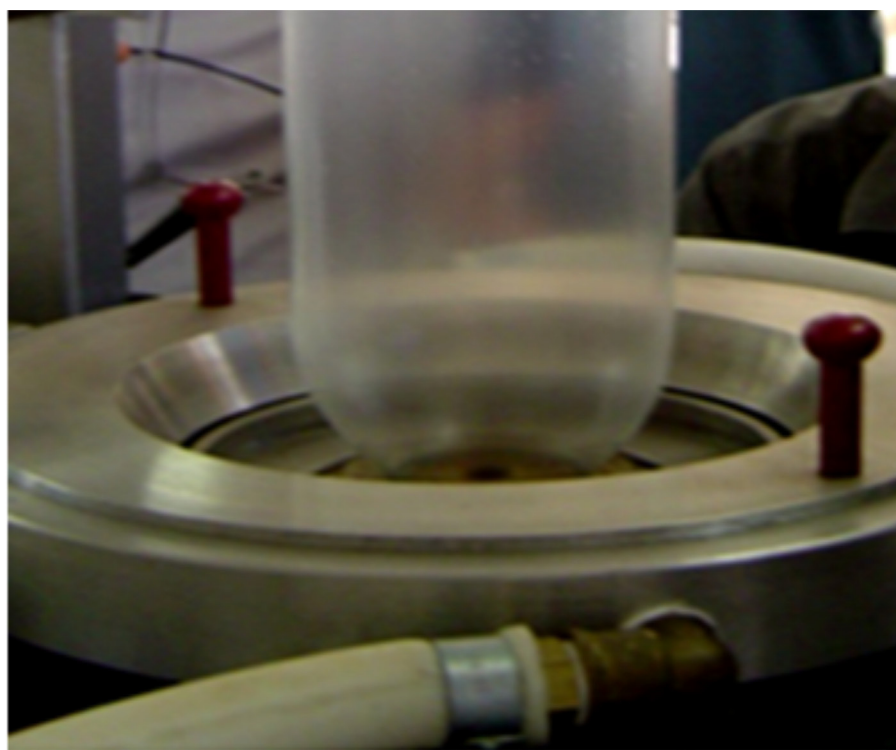


Figure 1S. Appearance of Na1.75% film during blow extrusion